

Photon Shot Noise Dephasing in the Strong-Dispersive Limit of Circuit QED

A. P. Sears, A. Petrenko, G. Catelani, L. Sun, Hanhee Paik, G.

Kirchmair, L. Frunzio, L. I. Glazman, S. M. Girvin, and R. J. Schoelkopf

Department of Physics and Applied Physics, Yale University, New Haven, Connecticut 06520, USA

(Dated: November 27, 2024)

We study the photon shot noise dephasing of a superconducting transmon qubit in the strong-dispersive limit, due to the coupling of the qubit to its readout cavity. As each random arrival or departure of a photon is expected to completely dephase the qubit, we can control the rate at which the qubit experiences dephasing events by varying *in situ* the cavity mode population and decay rate. This allows us to verify a pure dephasing mechanism that matches theoretical predictions, and in fact explains the increased dephasing seen in recent transmon experiments as a function of cryostat temperature. We investigate photon dynamics in this limit and observe large increases in coherence times as the cavity is decoupled from the environment. Our experiments suggest that the intrinsic coherence of small Josephson junctions, when corrected with a single Hahn echo, is greater than several hundred microseconds.

PACS numbers: 03.67.Lx, 42.50.Pq, 85.25

Solid-state superconducting quantum systems offer convenient and powerful platforms for quantum information processing. Rapid progress [1–3] is being made in engineering qubits and effectively isolating them from the surrounding electromagnetic environment. Despite these efforts, the measurement apparatus will always be used to contact the environment and is therefore a potential source for decoherence.

Recently [4] superconducting qubits have been created inside a three-dimensional (3D) resonator, leading to more than an order of magnitude increase in coherence time. Interestingly, the energy relaxation time T_1 has increased even more than the phase coherence time T_2^* , pointing to a new or newly important mechanism for dephasing [5]. These devices have a single Josephson junction, eliminating the sensitivity to flux noise [6], and surprisingly show only a weak temperature-dependent dephasing, inconsistent with some predictions based on extrapolations of junction critical current noise [7, 8]. In these devices, the qubit state is detected by observing the dispersive frequency shift of a resonant cavity. However, it is known [9–11] that in the strong-dispersive regime the qubit becomes very sensitive to stray cavity photons, which cause dephasing due to their random ac-Stark shift [12]. It requires increasing care to prevent this extrinsic mechanism from becoming the dominant source of dephasing as qubit lifetimes increase. Experiments elsewhere [13] and in our lab [14] have shown that pure dephasing times can be many hundreds of microseconds with careful thermalization and more extensive filtering.

In this Letter, we quantitatively test the dephasing of a qubit due to photon shot noise in the strong-dispersive coupling limit with a cavity. In this novel regime where the ac-Stark shift per photon is many times greater than the qubit linewidth γ and the cavity decay rate κ [15], the passage of any photon through the cavity performs a complete and unintended measurement of the qubit state. This limit also allows a precise determination of the photon number in the cavity using Rabi experiments on the photon number-split qubit spectrum [16]. With a simulated thermal bath injecting photons into the cav-

ity and *in situ* mechanical adjustment of the cavity κ , we find a pure dephasing of the qubit that quantitatively matches theory [10]. Furthermore, we verify that the qubit is strongly coupled to photons in several cavity modes and find that the dephasing from these modes accounts for the reduced coherence times as a function of cryostat temperature. Our measurements at 10 mK demonstrate that decreasing κ leads to longer qubit coherence times, suggesting that existing dephasing in superconducting qubits is due to unintended and preventable measurement by excess photons in higher frequency modes.

The experiments were performed (see Fig. 1) with a transmon qubit coupled in the strong-dispersive limit to a 3D cavity, and well approximated by the Hamiltonian [18]:

$$H_{\text{eff}}/\hbar = \omega_c a^\dagger a + (\omega_q - \chi a^\dagger a) b^\dagger b - \frac{\alpha}{2} b^\dagger b^\dagger b b, \quad (1)$$

where the operator a^\dagger creates a cavity photon and the operator b^\dagger creates a qubit excitation. Then ω_c is the cavity frequency, ω_q and α are the qubit frequency and anharmonicity, and $\chi/2\pi = 7$ MHz is the light shift per photon which can be 1000 times larger than the qubit linewidth of $\gamma/2\pi = 5 - 12$ kHz, and the cavity linewidth $\kappa/2\pi = 6 - 120$ kHz. The large dispersive shift leads to the well-resolved peaks in the qubit spectrum shown in Fig. 1c, allowing us to conditionally manipulate the qubit depending on the cavity photon number N [16]. Measuring the height of a given photon number-split qubit peak (or the amplitude of a Rabi oscillation at frequency $\omega_q - N\chi$) allows a direct determination of the probability $P(N)$ for the cavity to have a particular photon number.

Dephasing of the qubit can be caused by a random change in cavity photon number, which shifts the qubit energy by $\hbar\chi$ per photon and leads to a large rate of phase accumulation relative to γ . Then the pure dephasing rate γ_ϕ , obtained in a Ramsey experiment for the qubit, depends on the stability of the N photon cavity state. When the cavity is connected to a thermal bath, the probability $P(N)$ follows a system of

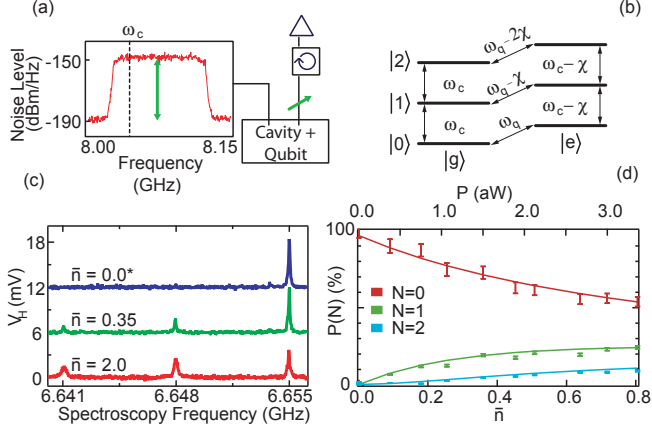


FIG. 1: (a) Experimental setup. Noise of varying amplitude at the cavity transition frequency is sent into the input port of a 3D resonator. The output port of the resonator has a movable coupler which varies the output side coupling quality factor Q_c from 1.0×10^5 to 2.5×10^7 . (b) Energy level diagram. The qubit has a transition frequency that is ac-Stark shifted by $-\chi$ for each photon in the cavity. (c) Photon number-splitting of the qubit spectrum. We inject noise and create a mean number \bar{n} of photons in the fundamental mode. The peaks correspond to $N = 0, 1, 2$ photons from right to left, with the cavity $Q = 1 \times 10^6$, and (*) even without applied noise we measure a photon occupation in the TE₁₀₁ mode of the cavity to be $\bar{n} \sim 0.02$. (d) Cavity population. Rabi experiments performed on each photon peak N for increasing noise power with cavity $Q = 2.5 \times 10^5$. The signal amplitude gives the probability of finding N photons in the cavity. Two linear scaling factors, fit globally, provide conversion from homodyne readout voltage [17] to probability (vertical axis), and from attowatts within the cavity bandwidth to \bar{n} (horizontal axis). Error bars represent 1σ fluctuations in the $|e\rangle$ state readout voltage. The solid lines are a thermal distribution using the fit scaling parameters.

equations [19] for the rate of change into and out of the N photon state: $dP(N)/dt = \kappa(\bar{n} + 1)(N + 1)P(N + 1) + \kappa\bar{n}NP(N - 1) - \Gamma_{\text{out}}P(N)$, where the cavity decay rate $\kappa = 1/\tau$ is the inverse of its decay time τ , \bar{n} is the average number of photons, and

$$\Gamma_{\text{out}} = \kappa[(\bar{n} + 1)N + \bar{n}(N + 1)] \quad (2)$$

combines the spontaneous emission of photons with the stimulated emission due to thermal photons. Then, in the strong-dispersive regime (and neglecting other sources of dephasing) the dephasing rate becomes $\gamma_\phi = \Gamma_{\text{out}}$, and the success of an experiment that relies on phase predictability of the qubit requires a constant photon number in the cavity throughout each cycle.

To verify this prediction for γ_ϕ quantitatively, we first calibrate our thermal bath and then obtain κ with experiments on the photon peaks of the qubit. We can determine the cavity decay rate κ by exciting the cavity with a short coherent pulse while measuring the repopulation of the ground state $|g, 0\rangle$ (i.e. the amplitude of the zero-photon Rabi oscillations) over timescale τ . Alternatively, exciting the cavity with a wideband noise source that covers the cavity ω_c transition frequency but

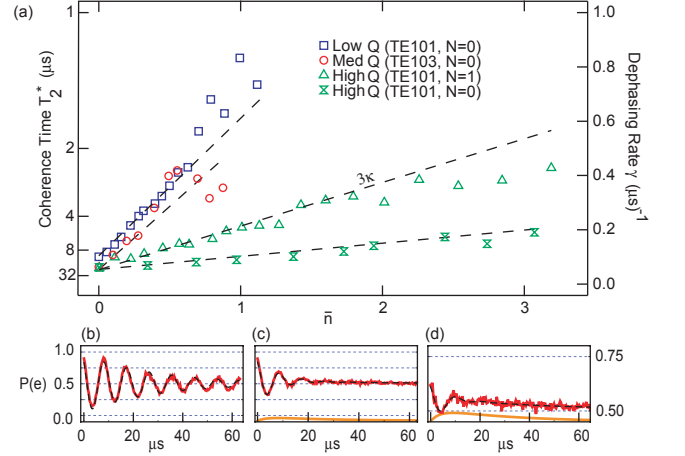


FIG. 2: Qubit dephasing due to photon noise. (a) Qubit coherence time, determined from Ramsey experiments on the $N = 0$ or $N = 1$ (\triangle) photon peaks, as a function of both cavity Q and \bar{n} . The dashed lines are theory, with an offset due to residual dephasing. Each has a slope proportional to κ (or 3κ for $N = 1$ experiments), according to Eq. 2. The (\circ) are coherence times vs. population in TE₁₀₃ mode, which also dephases the qubit. (b) Ramsey with no noise injected, fundamental mode $Q = 1 \times 10^6$, and $T_2^* = 26 \mu\text{s}$. The solid line is a fit with an exponentially decaying sine. (c) A Ramsey with moderate noise. Contrast and T_2^* are reduced. Fundamental mode $Q = 2.5 \times 10^5$, $\bar{n} = 0.25$, $T_2^* = 7.7 \mu\text{s}$. (d) Ramsey with high noise. Fundamental mode $Q = 1 \times 10^6$, $\bar{n} = 3.1$, $T_2^* = 5.2 \mu\text{s}$. Our selective ($N = 0$) pulses produce a loss of contrast and a non-oscillating signal addition (orange) as photon population returns to a thermal distribution. The dashed black line is a numerical simulation (see the Supplemental Materials).

not the qubit ω_q transition frequency, creates an average photon number $\bar{n} = AP_{BE}(T)Q/Q_c$. Here, A is the linear power loss from additional cold attenuation, $P_{BE} = 1/(e^{\hbar\omega/kT} - 1)$ is the Bose-Einstein population of the 50Ω load of the noise source at effective temperature T , located outside the cavity. The total cavity quality factor $Q = \omega\tau$ has an inverse which is the sum of the inverses of the coupling quality factor Q_c of the noise source port, all other port couplings, and the internal quality factor Q_{int} . In steady state and for uncorrelated noise, the probability $P(N)$ of finding the qubit in an environment with N photons is a thermal distribution $P(N) = \bar{n}^N/(\bar{n} + 1)^{(N+1)}$, as verified by the data in Fig. 1d. With these measurements we obtain the scaling of \bar{n} as a function of applied noise power for each different value of κ , allowing a comparison with Eq. 2 using no adjustable parameters.

To observe the influence of photon dephasing on our qubit, we test Eq. 2 over a wide range of values for both \bar{n} and κ as shown in Fig. 2. The photon number is varied by adjusting the attenuation following our noise source, while κ is controlled by retracting the resonator output coupler using a Kevlar string connected to the top of the fridge, exponentially increasing the Q_c as it is withdrawn. For large κ , photons enter and leave quickly, so long periods uninterrupted by a transit are

rare even if the average occupation is low, and the phase coherence time is short. In the Ramsey data shown in Fig. 2 the dephasing rate is universally proportional to injected \bar{n} and κ , with an offset due to spontaneous decay (if $N > 0$), and residual photons or other intrinsic dephasing. These experiments confirm our understanding of the qubit dephasing rate in the strong-dispersive limit, and point to the importance of excess photons or an effective temperature of a mode for qubit coherence.

Importantly, we use slow Gaussian pulses to control the qubit in order to exploit the photon-dependence of our Hamiltonian. With a width of $\sigma = 100$ ns, the narrow frequency span of the pulses means that Ramsey experiments add signal contrast only when the chosen photon number N has remained in the cavity throughout the experiment, a type of post-selection evident in the different scalings of Fig. 2b-d. Once conditioned, photon transitions during the experiment lead to an incoherent response in our qubit readout, when at a random point in time t_0 an initially prepared superposition changes: $|\psi(t_0)\rangle = 1/\sqrt{2}(|g,0\rangle + |e,0\rangle) \rightarrow |\psi(t)\rangle = 1/\sqrt{2}(|g,1\rangle + \exp[i\chi(t-t_0)]|e,1\rangle)$ for time $t > t_0$. Our qubit readout [17] traces over all photon states, and the unknown final phase of the superposition produces a decay in the Ramsey fringes, as the experiment records the qubit excitation despite any cavity transition. Additionally, a characteristic bump and slope are visible in the data and must be removed before fitting the Ramsey signal with the usual decaying sine function. These features can be understood as the re-equilibration of the cavity photon number after the first qubit manipulation conditionally prepares a certain photon number, and are well fit (see Fig. 3 of the Supplement) by a simple master equation which includes the incoherent cavity drive as well as qubit and cavity decay.

While the fundamental TE_{101} mode of our 3D resonator serves both as the qubit readout channel and as a mechanism for dephasing, the rectangular cavity in fact supports a set of TE_{10n} modes [20] whose influence we must consider. Then a more comprehensive Hamiltonian than Eq. 1 must incorporate many different cavity frequencies, each with a coupling strength that depends on antenna length and the positioning of the qubit in the cavity [18]. This coupling g_n is large for odd- n TE_{10n} modes where the electric field has an antinode at the qubit, while the even- n modes have greatly diminished coupling to the qubit due to a node along the qubit antenna. For our parameters, the fundamental TE_{101} mode $\omega_1/2\pi = 8.01$ GHz, $\omega_q/2\pi = 6.65$ GHz, and $g_1/2\pi = 127$ MHz, the qubit anharmonicity $\alpha = 340$ MHz leads to an ac-Stark shift of $\chi_1/2\pi = 7$ MHz. Similarly, the first odd harmonics TE_{103} with $\omega_3 = 12.8$ GHz has a large $\chi_3/2\pi = 1$ MHz. In fact, with this mode we can perform high fidelity readout, measure the photon mode population (using longer $\sigma = 800$ ns width pulses), and observe its influence on decoherence by injecting noise near ω_3 . In general, we should consider *all* cavity modes that have a non-zero coupling to the qubit as sources of significant decoherence. For example, the odd- n TE_{10n} modes at frequency ω_n and detuning $\Delta_n = \omega_n - \omega_q$, have a coupling

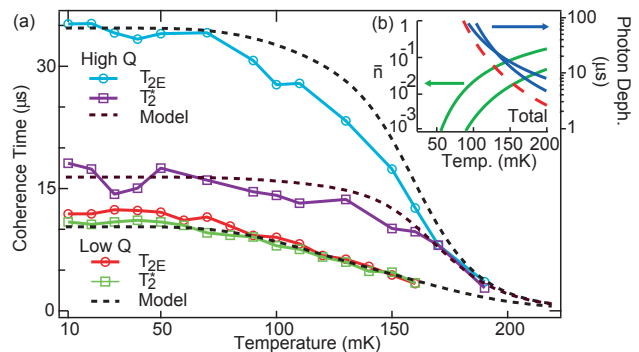


FIG. 3: (a) Decoherence due to thermal photons. The coherence times extracted from Ramsey (T_2^*) and Hahn echo (T_{2E}) experiments measured as a function of cryostat temperature. To model dephasing (dashed lines), we predict population in the TE_{101} and TE_{103} modes of the cavity. Then, we sum the total dephasing rate using the measured quality factors for each mode (High Q : $\tau_{101} = 20$ μ s, $\tau_{103} = 4$ μ s; Low Q : $\tau_{101} = 2$ μ s, $\tau_{103} = 400$ ns). For high Q , the use of a Hahn echo pulse leads to a large T_{2E} because either the photon state has much longer correlation time or the remaining dephasing similarly occurs at low frequencies. Although the decline in T_1 (not shown) [21] contributes to the trend, population in both TE_{101} and TE_{103} are needed for a good fit. (b) Bose-Einstein population of the first two odd- n TE_{10n} modes at 8 and 12.8 GHz (green) and the coherence limits they impose individually (blue) and collectively (dashed red) for the low Q values measured above.

$g_n \propto \sqrt{\omega_n}$ and an ac-Stark shift $\chi_n = g_n^2 \alpha / \Delta_n (\Delta_n + \alpha)$ which decrease only slowly as $1/n$. Consequently, there may be many modes with significant dispersive shifts that can act as sources of extrinsic qubit decoherence. Moreover, since the coupling quality factors of these modes typically decreases with frequency, even very small photon occupancies (which are usually ignored, not measured or as carefully filtered) must be suppressed to obtain maximum coherence.

The photon shot noise from multiple cavity modes provides a simple explanation for the anomalous qubit dephasing previously observed [4] as a function of cryostat temperature. In this case, each cavity mode should be populated with the Bose-Einstein probability P_{BE} and these thermal photons can make an unintended measurement of the qubit, disrupting phase-sensitive experiments. The predicted occupancies for the TE_{101} and TE_{103} modes are shown (green lines) in the inset of Fig. 3, along with their predicted dephasing (blue lines). Having confirmed the dephasing rates for all modes individually we can now combine the effect of all modes that strongly couple to the qubit: $\gamma_\phi = \sum \bar{n}_i \kappa_i$. This total thermal decoherence rate is shown as the red dashed line in the inset of Fig. 3, for typical parameters. Since these modes have $\hbar\omega_n \gg k_B T$, the predicted dephasing time is in excess of 100 microseconds below 80 mK due to the exponentially suppressed number of blackbody photons. However, since any particular mode coupling to the qubit in the strong-dispersive limit may have a relatively fast decay time τ , even very small ($\sim 10^{-3} - 10^{-2}$) non-thermal populations \bar{n} could easily satisfy $\bar{n}\kappa \gg 1/2T_1$, limiting the coherence through pure dephas-

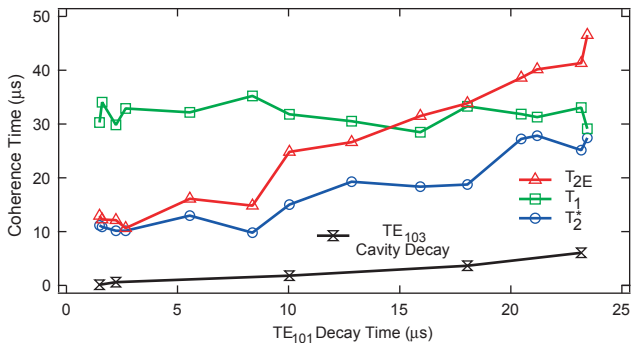


FIG. 4: Coherence times versus TE_{101} mode decay τ . The TE_{103} cavity, which naturally decays more strongly through the couplers, increases in Q as the entire resonator is decoupled from our coaxial lines. While T_1 is nearly constant due to the large qubit detuning from the cavity, its T_2^* and T_{2E} increase as the coupling pin is withdrawn from the 3D resonator. This is consistent with diminishing dephasing from cavity modes with $\kappa < \chi$, where a photon transit strongly measures [11] the qubit state.

ing alone to $T_2^* \approx 1/\gamma_\phi = \tau/\bar{n}$. The measured coherence times as a function of temperature are well fit (see Fig. 3) by the combined dephasing of thermal occupancy of the TE_{101} and TE_{103} modes, plus a parameter adjusted to represent the residual dephasing in each experiment. This excess could be due to another mechanism intrinsic to the qubit, or simply due to insufficient filtering or thermalization of the apparatus, leading to a small non-thermal photon population.

Further evidence that the true intrinsic coherence limits of the 3D transmons have not yet been observed is provided by the data shown in Fig. 4, where the qubit relaxation time (T_1), Ramsey time (T_2^*), and Hahn echo time (T_{2E}) at 10 mK are shown as a function of the TE_{101} cavity decay time. We see that the relaxation time is relatively unaffected by cavity lifetime, since this qubit is sufficiently detuned from the cavity to minimize the Purcell effect [1]. However, we observe a general trend where T_2^* and T_{2E} increase as the cavity lifetime increases. This is consistent with a decoherence due to residual photons with ever slower dynamics, but *not* expected due to e.g. junction critical current noise, which should be independent of cavity properties. The maximum echo time ($45 \mu\text{s} \approx 1.5 T_1$) observed here indicates that coherence of small Josephson junction qubits is in excess of several hundred microseconds when corrected by a single Hahn echo.

In conclusion, we have performed experiments involving precise thermal photon populations to quantitatively induce qubit dephasing in good agreement with simple theory. We find that photons in the fundamental and at least one harmonic mode of the cavity strongly couple to a transmon qubit and note that at the nominal base temperature of our cryostat they produce a negligible amount of dephasing. However, the sensitivity of the qubit to photons at many frequencies requires that we either keep all modes of the cavity in their ground state, or else minimize the influence of non-thermal popula-

tions by reducing their measurement rate [22]. Inclusion of the cavity harmonics in dephasing calculations leads to an understanding of the earlier, anomalous, temperature-dependent decoherence in our devices [4]. Finally, we find evidence that interactions with the residual photons in our 3D cavity likely mask the intrinsic coherence time of the Josephson junction, whose limits are much longer than qubit coherence times seen so far. As qubit linewidths shrink in the future, other effects such as quasiparticle parity [23–25] or nuclear spins [26] may further split the qubit spectrum, enabling probes of their state dynamics using these procedures.

We thank Michel Devoret for valuable discussions. L. F. acknowledges partial support from CNR-Istituto di Cibernetica. This research was funded by the Office of the Director of National Intelligence (ODNI), Intelligence Advanced Research Projects Activity (IARPA), through the Army Research Office, as well as by the National Science Foundation (NSF DMR-1004406). All statements of fact, opinion or conclusions contained herein are those of the authors and should not be construed as representing the official views or policies of IARPA, or the U.S. Government.

-
- [1] A. Houck, J. Schreier, B. Johnson, J. Chow, J. Koch, J. Gambetta, D. Schuster, L. Frunzio, M. Devoret, S. Girvin, et al., *Phys. Rev. Lett.* **101**, 080502 (2008).
 - [2] M. Neeley, M. Ansmann, R. Bialczak, M. Hofheinz, N. Katz, E. Lucero, A. O’Connell, H. Wang, A. N. Cleland, and J. M. Martinis, *Phys. Rev. B* **77**, 180508(R) (2008).
 - [3] M. Steffen, F. Brito, D. DiVincenzo, S. Kumar, and M. Ketchen, *New J. Phys.* **11**, 033030 (2009).
 - [4] H. Paik, D. Schuster, L. Bishop, G. Kirchmair, G. Catelani, A. Sears, B. Johnson, M. Reagor, L. Frunzio, L. Glazman, et al., *Phys. Rev. Lett.* **107**, 240501 (2011).
 - [5] A. A. Houck, J. Koch, M. H. Devoret, S. M. Girvin, and R. J. Schoelkopf, *Quantum Inf. Process.* **8**, 105 (2009).
 - [6] F. C. Wellstood, C. Urbina, and J. Clarke, *Appl. Phys. Lett.* **50**, 772 (1987).
 - [7] D. Van Harlingen, T. Robertson, B. Plourde, P. Reichardt, T. Crane, and J. Clarke, *Phys. Rev. B* **70**, 064517 (2004).
 - [8] J. Eroms, L. C. van Schaarenburg, E. F. C. Driessen, J. H. Plantenberg, C. M. Huizinga, R. N. Schouten, A. H. Verbruggen, C. J. P. M. Harmans, and J. E. Mooij, *Appl. Phys. Lett.* **89**, 122516 (2006).
 - [9] P. Bertet, I. Chiorescu, G. Burkard, K. Semba, C. Harmans, D. DiVincenzo, and J. Mooij, *Phys. Rev. Lett.* **95**, 257002 (2005).
 - [10] J. Gambetta, A. Blais, D. Schuster, A. Wallraff, L. Frunzio, J. Majer, M. Devoret, S. Girvin, and R. Schoelkopf, *Phys. Rev. A* **74**, 042318 (2006).
 - [11] I. Serban, E. Solano, and F. K. Wilhelm, *Europhysics Letters (EPL)* **80**, 40011 (2007).
 - [12] D. Schuster, A. Wallraff, A. Blais, L. Frunzio, R. Huang, J. Majer, S. Girvin, and R. Schoelkopf, *Phys. Rev. Lett.* **94**, 123602 (2005).
 - [13] C. Rigetti, S. Poletto, J. Gambetta, B. Plourde, J. Chow, A. Corcoles, J. Smolin, S. Merkel, J. Rozen, G. Keefe, et al., *Arxiv preprint arXiv:1202.5533* (2012).

- [14] L. Sun and A. Petrenko, in prep.
- [15] D. I. Schuster, A. A. Houck, J. A. Schreier, A. Wallraff, J. M. Gambetta, A. Blais, L. Frunzio, J. Majer, B. Johnson, M. H. Devoret, et al., *Nature* **445**, 515 (2007).
- [16] B. R. Johnson, M. D. Reed, A. A. Houck, D. I. Schuster, L. S. Bishop, E. Ginossar, J. M. Gambetta, L. DiCarlo, L. Frunzio, S. M. Girvin, et al., *Nature Phys.* **6**, 663 (2010).
- [17] M. Reed, L. DiCarlo, B. Johnson, L. Sun, D. Schuster, L. Frunzio, and R. Schoelkopf, *Phys. Rev. Lett.* **105**, 173601 (2010).
- [18] S. Nigg, H. Paik, B. Vlastakis, G. Kirchmair, S. Shankar, L. Frunzio, M. Devoret, R. Schoelkopf, and S. Girvin, Arxiv preprint:1204.0587 (2012), *Phys. Rev. Lett.* in press.
- [19] D. F. Walls and G. J. Milburn, *Quantum optics* (Springer, Berlin; New York, 1994), ISBN 3540588310.
- [20] C. P. Poole, *Electron spin resonance : a comprehensive treatise on experimental techniques* (Wiley, New York [u.a.], 1967), ISBN 9780470693865.
- [21] G. Catelani, J. Koch, L. Frunzio, R. Schoelkopf, M. Devoret, and L. Glazman, *Phys. Rev. Lett.* **106**, 077002 (2011).
- [22] M. Hatridge and S. Shankar, in prep.
- [23] J. Schreier, A. Houck, J. Koch, D. Schuster, B. Johnson, J. Chow, J. Gambetta, J. Majer, L. Frunzio, M. Devoret, et al., *Phys. Rev. B* **77**, 180502(R) (2008).
- [24] L. Sun, L. DiCarlo, M. Reed, G. Catelani, L. S. Bishop, D. I. Schuster, B. R. Johnson, G. A. Yang, L. Frunzio, L. Glazman, et al., Arxiv preprint:1112.2621 (2012), *Phys. Rev. Lett.* in press.
- [25] O. Naaman and J. Aumentado, *Phys. Rev. B* **73**, 172504 (2006).
- [26] D. Schuster, A. Sears, E. Ginossar, L. DiCarlo, L. Frunzio, J. Morton, H. Wu, G. Briggs, B. Buckley, D. Awschalom, et al., *Phys. Rev. Lett.* **105**, 140501 (2010).

Supplemental Material for
Photon Shot Noise Dephasing in the Strong-Dispersive Limit of Circuit QED

A. P. Sears, A. Petrenko, G. Catelani, L. Sun, H. Paik, G. Kirchmair,
 L. Frunzio, L. I. Glazman, S. M. Girvin, and R. J. Schoelkopf

¹*Department of Physics and Applied Physics, Yale University, New Haven, Connecticut 06520, USA*

(Dated: June 6, 2012)

I. EXPERIMENTAL APPARATUS

The experiment involved a two port 3D resonator with qubit J3, previously reported [1] to have $T_1 = 42 \mu\text{s}$, and $T_2^* = T_{2E} = 12 \mu\text{s}$ with a fundamental cavity quality factor $Q \sim 3.2 \times 10^5$. We placed the aluminum 3D resonator at the 10 mK base plate of a dilution cryostat, attached to a brass translation stage and the copper cold finger of the cryostat. On the input side of the resonator, coax lines were attenuated first by 20 dB at the 4 K stage, then at the base plate by a -20 dB directional coupler followed by 10 dB of resistive attenuation before the input port to the cavity, similar to our previous experiments (see Fig. 1). The output side coupler was attached via a Kevlar string, heatsunk at several stages, to a linear feedthrough at the top of the cryostat. With this we were able to translate the coupler stage by up to 3 mm. Hand-formable UT-85 coax cables allow the output coupler to be pulled out of the cavity, while a BeCu spring provides a restoring force. This varies the coupling quality factor Q_c of the port from $1 \times 10^5 - 3 \times 10^7$, while the input coupler is fixed with coupling quality factor $Q_{\text{in}} = 1 \times 10^7$. After the output coupler but still at the base plate, two non-reciprocal isolators attenuated Nyquist-Johnson noise from the wideband HEMT amplifier mounted at 4 K while permitting transmission of the readout signal. At room temperature, the signal was mixed down to 10 MHz after further amplification.

II. RABI EXPERIMENTS ON PHOTON PEAKS

In order to determine the thermal \bar{n} occupation of a cavity mode, we perform a set of power Rabi experiments, varying the power of a single Gaussian pulse of fixed duration applied to one of the N photon qubit peaks. The qubit readout signal after a photon selective qubit π -pulse is proportional to the difference in qubit excited and ground state population $P(e, N) - P(g, N)$. In Fig. 2 each graph contains a power Rabi dataset for $N = 0, 1$, and 2, for a different mean number of photons \bar{n} injected into the cavity. The oscillating signal amplitude in a trace is a lock-in measurement of the probability for the cavity to be occupied by N photons. Each power Rabi measurement provides a data point in Fig. 1d of the main text, with axes for \bar{n} (horizontal) and $P(N)$ (vertical) that have been scaled by the optimal two parameters which fit the whole data set to a thermal distribution. Repeated datasets analyzed by the same procedure yielded an \bar{n} scaling parameter that varied by $\pm 5\%$.

Additionally, we found $P(e, 0) = 5 \pm 1\%$ throughout the experiment, a phenomenon which is not unique [2] among 3D superconducting qubits but also not yet completely understood. To obtain this value we compare the contrast of power Rabi experiments on the excited qubit peak at $\omega_q - \alpha$, with and without an initial π inversion on the qubit, similar to measurements

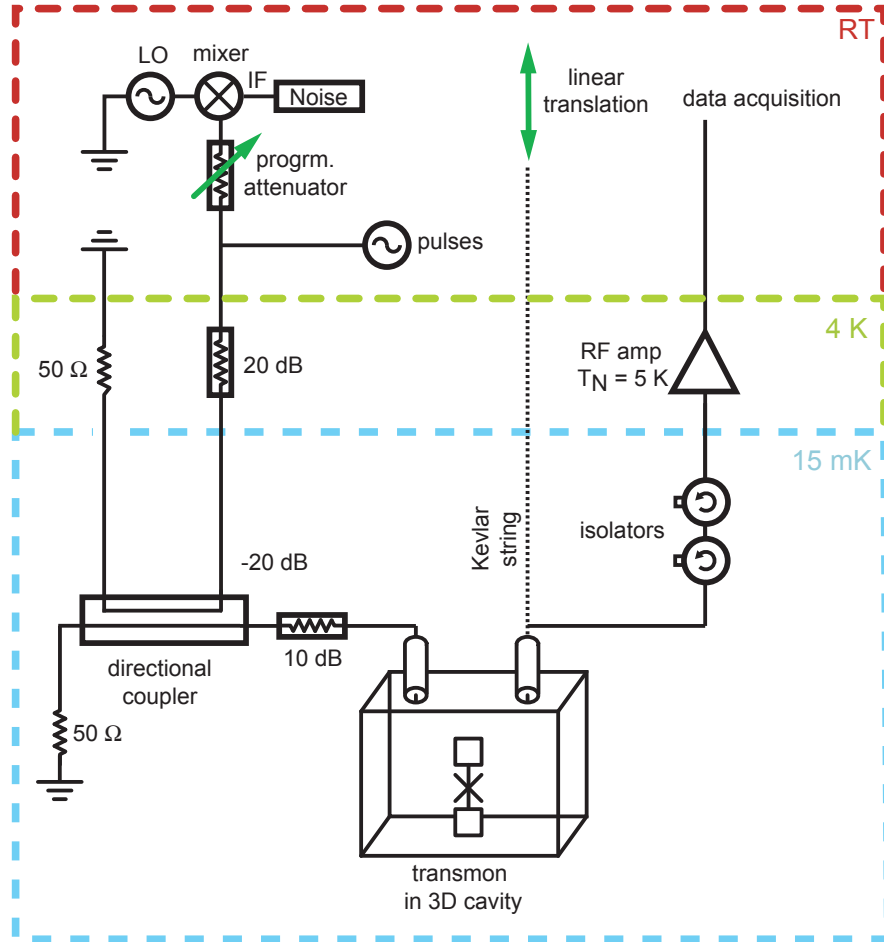


FIG. 1: Block diagram of the measurement setup.

of cavity photon population. Since our noise source covers even the cavity transitions that have shifted due to the excited qubit state (the state dependent shift), this is not expected to interfere with our quantitative measurements of dephasing. We also find (see Fig. 2*) even without applied noise we measure a photon occupation in the TE_{101} mode of the cavity to be $\bar{n} \sim 0.02$.

III. RAMSEY SIGNAL

In this section we give a brief explanation of the procedure used to fit the Ramsey experiments. The energy level diagram in Fig. 1b of the main text can be interpreted as showing that for a given qubit state the cavity is effectively a harmonic oscillator

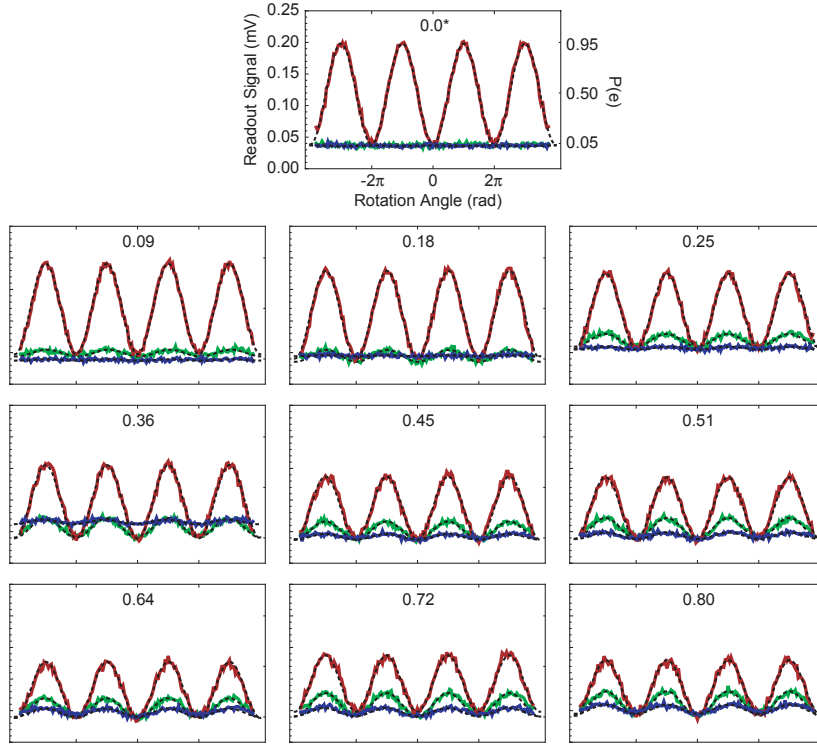


FIG. 2: Rabi experiments on the TE_{101} photon number-split qubit. For each curve the qubit Rabi pulse is on a different peak, from $N = 0$ (red) to $N = 1$ (green) and $N = 2$ (blue). The vertical scale is the integrated readout signal, and in all graphs $P(0) > P(1) > P(2)$. All graphs have the same axes, and the cavity Q is 2.5×10^5 .

with frequency ω_c , or $\omega_c - \chi$ when the qubit is excited. Assuming long qubit relaxation time $T_1 \gg 1/\kappa$, the qubit does not relax during the evolution of the cavity occupation. Then for a given qubit state the dynamics of the probability $P(N, t)$ of having N photons in the cavity at time t is governed by the rate equations:

$$\frac{dP(N)}{dt} = \kappa(\bar{n}+1)(N+1)P(N+1) + \kappa\bar{n}NP(N-1) - \kappa[\bar{n}(N+1) + (\bar{n}+1)N]P(N) \quad (1)$$

and the steady-state probability $P_s(N)$ is

$$P_s(N) = \frac{1}{1+\bar{n}} \left(\frac{\bar{n}}{1+\bar{n}} \right)^N \quad (2)$$

With the qubit initially in the ground state, a $\pi/2$ pulse at the $N = 0$ peak will coherently split the occupation probability between ground and excited states. This means that the initial probability distribution after the $\pi/2$ pulse is

$$P(N, 0) = \begin{cases} \frac{1}{2} \frac{1}{1+\bar{n}}, & N = 0 \\ 0, & N > 0 \end{cases} \quad (3)$$

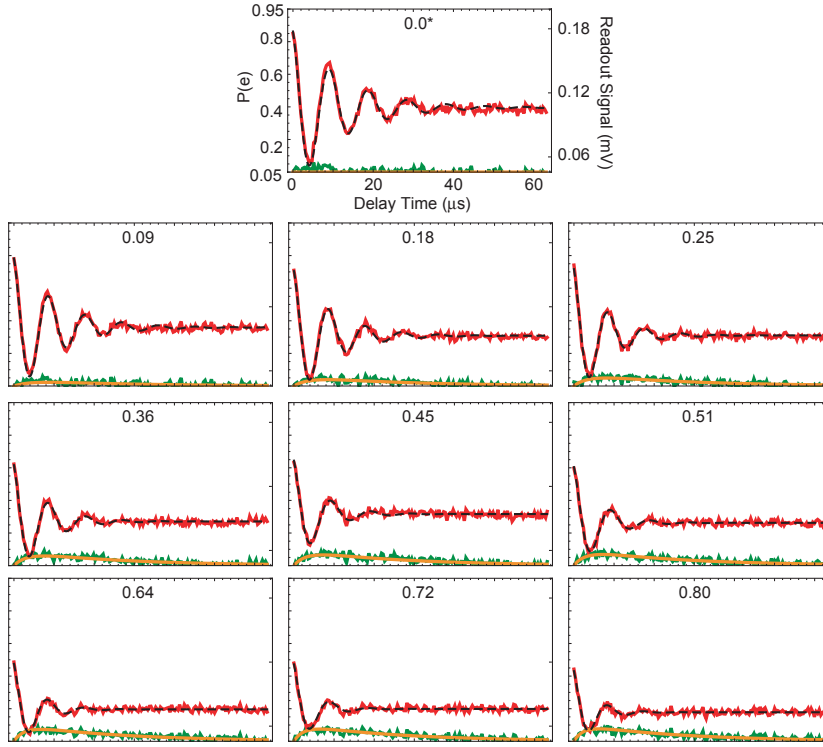


FIG. 3: A set of Ramsey experiments similar to those used for series in Fig. 2 of the main text. Each graph has the same axes and is labelled by the \bar{n}_{eff} , as calibrated by the Rabi thermometry experiments. The adjusted data (red) has had the incoherent readout response (orange) subtracted from the readout signal, before being fit with an exponentially decay sine (dashed). Additionally, the original data after subtracting the final fitted decaying sine is shown (green). The cavity Q is 2.5×10^5 .

After the second $\pi/2$ pulse at time t_f , the probability distribution for $N > 0$ is simply $P(N, t_f)$ as determined by the evolution of $P(N, t)$ from the above initial conditions, while $P(0, t_f)$ is the usual Ramsey fringe signal [3] which we denote $S_R(t_f)$, exhibiting decay times which scale according to $1/\bar{n}\kappa$ (see Fig. 2 of the main text). As the readout sums over all photon number states, the signal $S(t_f)$ is

$$S(t_f) = S_R(t_f) + P_B(t_f) \quad (4)$$

with the “bump” P_B defined as

$$P_B(t_f) = \sum_{N>0} P(N, t_f). \quad (5)$$

To fit the signal, we need to calculate the function $P_B(t)$. This can be done by solving the rate equations (1) with the initial

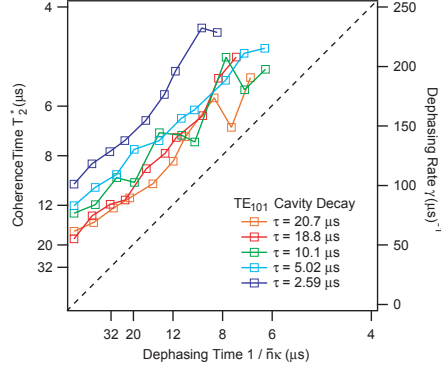


FIG. 4: Universal Dephasing Plot: an alternative presentation of our measurements of qubit dephasing versus noise. Here the horizontal axis is $\bar{n}\kappa$, scaled for each trace, which according to Eq. 2 from the main text we expect to be equal to T_ϕ for the qubit. The vertical offsets correspond to residual dephasing even for $\bar{n} = 0$, evident in Fig. 4 in the main text.

conditions (3). An analytical solution will be given elsewhere. Here we simply give the final answer,

$$P_B(t) = \frac{1}{2} \frac{\bar{n}}{(1+\bar{n})^2} \frac{1 - e^{-\kappa t}}{1 - \frac{\bar{n}}{1+\bar{n}} e^{-\kappa t}} \quad (6)$$

So far we have ignored the qubit and its relaxation. A more detailed analysis gives a reduction of the amplitude of the bump (which we account for with the factor M in Eq. 8 below) and its relaxation over the T_1 time scale. Then the actual signal is given by

$$S(t_f) = S_R(t_f) + S_B(t_f) \quad (7)$$

with

$$S_B(t_f) = M P_B(t_f) e^{-t_f/T_1}, \quad (8)$$

consistent with the dashed curves in Fig. 3 and in the main text.

We account for this signal with the following process. First we simulate the system using values obtained via experiment: cavity decay time τ , and \bar{n} obtained through calibration. Then, we take the expected $S_B(t_f)$ (the excited qubit population with $N > 0$) and remove it from the Ramsey signal, fitting the remainder to a decaying exponential. This typically leads to a correction to γ that is $\sim 10 - 30\%$. The products of this process are shown for a series with the same $\kappa = 1/\tau$ as that in Fig. 2 here, and Fig. 1d of the main text.

IV. COUPLED BATHS

When the resistor component of an isolated RLC circuit is at finite temperature, the harmonic oscillator mode has non-zero population $\bar{n} = P_{BE}(T)$, the Bose-Einstein occupation at the mode frequency. If other baths are coupled with the oscillator,

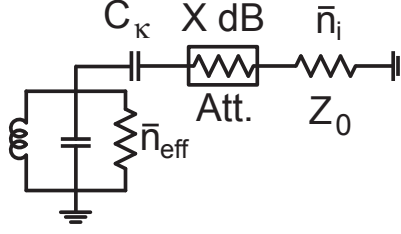


FIG. 5: A harmonic oscillator is coupled via a port to a thermal load, which populates the mode with \bar{n} .

then it experiences a total rate of excitation: $\Gamma_{\uparrow} = \sum \bar{n}_i \kappa_i$ where κ_i for our system includes both input and output pin couplers and an additional port representing internal dissipation, while the decay rate of any population in the oscillator is $\kappa = \sum \kappa_i$. In Fig. 5 we present this as a capacitive coupling C_{κ} to a resistor, where we can approximate [4] $\kappa_c = \omega (C_{\kappa} \omega)^2 Z_0 Z_{\text{int}}$ for a resonator with characteristic impedance Z_{int} . When a cold attenuator with dissipation X in dB is inserted between a port and its thermal load, this effectively reduces $P_{\text{BE}}(T)$ by $A = 10^{-X/10}$, the linear power reduction amount [5] of the attenuator. Then in the steady state $\sum \bar{n}_i \kappa_i = \bar{n}_{\text{eff}} \kappa$, or $\bar{n}_{\text{eff}} = \sum \bar{n}_i \kappa_i / \sum \kappa_i$, where \bar{n}_{eff} is the mean photon number due to thermal or injected noise. For a single external bath at temperature T , the only non-zero \bar{n}_i is injected through the port with decay rate κ_c , giving $\bar{n}_{\text{eff}} = AP_{\text{BE}}(T) \kappa_c / \kappa = AP_{\text{BE}}(T) Q / Q_c$ as in the main text.

-
- [1] H. Paik, D. Schuster, L. Bishop, G. Kirchmair, G. Catelani, A. Sears, B. Johnson, M. Reagor, L. Frunzio, L. Glazman, et al., *Phys. Rev. Lett.* **107**, 240501 (2011).
- [2] A. D. Corcoles, J. M. Chow, J. M. Gambetta, C. Rigetti, J. R. Rozen, G. A. Keefe, M. Beth Rothwell, M. B. Ketchen, and M. Steffen, *Appl. Phys. Lett.* **99**, 181906 (2011).
- [3] N. Ramsey, *Molecular beams* (Clarendon Press ; Oxford University Press, Oxford; New York, 1985), ISBN 0198520212.
- [4] M. Goppl, A. Fragner, M. Baur, R. Bianchetti, S. Filipp, J. M. Fink, P. J. Leek, G. Puebla, L. Steffen, and A. Wallraff, *J. Appl. Phys.* **104**, 113904 (2008).
- [5] F. Pobell, *Matter and methods at low temperatures* (Springer-Verlag, Berlin; New York, 1996), ISBN 3540585729.